Identification of Vascular Breast Tumor Markers by Laser Capture Microdissection and Label-Free LC-MS

ARTICLE *in* JOURNAL OF PROTEOME RESEARCH · MARCH 2011

Impact Factor: 4.25 · DOI: 10.1021/pr101267k · Source: PubMed

9 AUTHORS, INCLUDING:

Jennifer J Hill
National Research Council Canada
12 PUBLICATIONS **911** CITATIONS
SEE PROFILE

Tammy-Lynn Tremblay
National Research Council Canada
13 PUBLICATIONS **506** CITATIONS
SEE PROFILE

Anne E G Lenferink
National Research Council Canada
39 PUBLICATIONS **1,703** CITATIONS
SEE PROFILE

Edwin Wang
National Research Council Canada
73 PUBLICATIONS **2,031** CITATIONS
SEE PROFILE

Journal of proteome research

ARTICLE

pubs.acs.org/jpr

Identification of Vascular Breast Tumor Markers by Laser Capture Microdissection and Label-Free LC−MS

Jennifer J. Hill,*[,†] Tammy-Lynn Tremblay,[†] Ally Pen,[†] Jie Li,[‡] Anna C. Robotham,[†] Anne E. G. Lenferink,[‡] Edwin Wang,[‡] Maureen O'Connor-McCourt,[‡] and John F. Kelly[†]

[†]Institute for Biological Sciences, National Research Council Canada, 100 Sussex Drive, Ottawa, Ontario, Canada

[‡]Biotechnology Research Institute, National Research Council Canada, 6100 Royalmount Avenue, Montreal, Quebec, Canada

Supporting Information

ABSTRACT: Blood vessels in tumors frequently show abnormal characteristics, such as tortuous morphology or leakiness, but very little is known about protein expression in tumor vessels. In this study, we have used laser capture microdissection (LCM) to isolate microvessels from clinical samples of invasive ductal carcinoma (IDC), the most common form of malignant breast cancer, and from patient-matched adjacent nonmalignant tissue. This approach eliminates many of the problems associated with the heterogeneity of clinical tumor tissues by controlling for differences in protein expression between both individual patients and different cell types. Proteins from the microvessels were trypsinized and the resulting peptides were quantified by a label-free nanoLC−MS method. A total of 86 proteins were identified that are over-expressed in tumor vessels relative to vessels isolated from the adjacent nonmalignant tissue. These proteins include well-known breast tumor markers such as Periostin and Tenascin C but also proteins with lesser-known or emerging roles in breast cancer and tumor angiogenesis (i.e., Serpin H1, Clic-1, and Transgelin 2). We also identified 40 proteins that were relatively under-expressed in IDC tumor vessels, including several components of the basement membrane whose lower expression could be responsible for weakening tumor vessels. Lastly, we show that a subset of 29 proteins, derived from our list of differentially expressed proteins, is able to predict survival in three publicly available clinical breast cancer microarray data sets, which suggests that this subset of proteins likely plays a functional role in cancer progression and outcome.

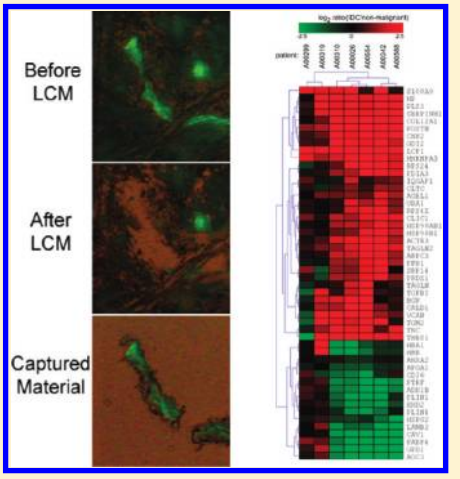

KEYWORDS: cancer, vessels, laser capture microdissection, invasive ductal carcinoma

INTRODUCTION

Worldwide, over 1 million breast cancer cases are diagnosed each year, accounting for nearly a quarter of all cancer incidences in women. Approximately 400 000 deaths are reported annually that can be directly attributed to this disease.[1] The majority of invasive breast cancers, approximately 80%, are generally classified as invasive ductal carcinomas (IDC), a malignant neoplasm that is initiated in the ductal lobes and then invades the surrounding breast tissue.

Tumor growth, invasion and metastasis are dependent on access to the blood supply. Blood vessel formation in tumors occurs by a variety of mechanisms including angiogenesis, a complex process by which existing blood vessels sprout and develop new vessels.[2−4] Angiogenesis is regulated by a balance of pro- and antiangiogenic factors and is normally restricted to developing or reproductive tissues and to wound repair. However, in tumors, angiogenesis is triggered by factors such as vascular endothelial growth factor (VEGF) that are secreted by hypoxic tumors and surrounding stromal cells, as well as by inflammatory cells recruited to the tumor site.[2,5−7] The process of tumor angiogenesis results in vessels that are structurally and functionally abnormal.[5] Relative to the normal vasculature, tumor vessels are leaky, tortuous, excessively branched and have many dead end sacs. Thus, despite the extensive vascularization observed in many tumors, perfusion is poor and a hypoxic environment is perpetuated within regions of the tumor.[5]

Proteomic studies of breast cancer abound but relatively few have focused on either the tumor microenvironment[8,9] or the tumor microvasculature.[10−12] Since the local environment often dictates protein expression in vessels, it is important to analyze the proteomes of vessels in the tumor tissue itself. This poses a challenge as vessels comprise a relatively small part of any tissue, even highly vascularized tumors. Therefore, a vessel enrichment/isolation strategy is required prior to protein extraction and analysis.

Laser capture microdissection (LCM) can be used to selectively isolate defined cellular features from tissues.[13] For example, several groups have used LCM to isolate tumor cells, epithelial cells, or metastases from clinical breast samples.[9,14,15] For

Received: December 21, 2010
Published: March 14, 2011

isolating microvessels, LCM has been used in a number of microarray-based genomic studies. Pen et al. compared the transcriptome of LCM-captured-vessels from malignant glioblastoma multiforme and nonmalignant brain tumors and found that 42 genes were differentially expressed.[16] Bhati et al. compared the transcriptome of LCM-captured vessels from luminal-A breast cancers and normal breast tissues.[17] They identified over 1176 differentially expressed genes, many of which code for extracellular matrix proteins.

There are still only a few examples of proteomic analyses being performed on LCM-captured microvessels, with the majority of studies focusing on brain microvessels.[18] In our laboratory, ICAT-LC-MS was used to analyze protein expression in LCM-captured microvessels from the brain of rats undergoing cerebral ischemia.[19] Over 3000 peptide pairs were detected and 55 proteins were found to be differentially expressed in ischemic vessels relative to normal. More recently, Lu et al. identified over 880 proteins from LCM-captured microvessels from mouse brain using 1D SDS-PAGE fractionation and LC-FTICR-MS/MS analysis.[20] Mustafa et al. employed MALDI-FTMS to analyze tryptic digests of microvessels LCM-captured from 10 human glioblastoma samples and 10 normal brain samples.[11] Three proteins, fibronectin, colligin-2 and acidic calponin-3, were determined to be strongly up-regulated in glioblastoma vessels.

In this article, we present the results of a study that compared protein expression in microvessels isolated by LCM from IDC breast tumors and adjacent nonmalignant breast tissue from the same patient. This approach has the advantage of eliminating some of the inherent heterogeneity between individual patients[21,22] and between different cell types present in the samples. A simple on-cap tryptic digestion procedure was developed to minimize issues arising from excessive sample manipulation postcapture. The resulting digests were analyzed by label-free LC−MS(/MS) and differential expression analysis was performed using software developed in-house. To our knowledge, this is the first proteomic study to use laser capture microdissection to enrich microvessels from clinical breast tumor samples.

METHODS

Materials

Clinical samples (10 frozen human breast tumor biospecimens and their matching adjacent nontumor control tissues) were provided by the Ontario Tumor Bank (OTB; Toronto, ON, Canada), which is funded by the Ontario Institute for Cancer Research. Specimens were selected using the following criteria: (1) Infiltrating Ductal Carcinoma (IDC) histology, (2) availability of nonmalignant adjacent breast tissue, (3) gender (female), (4) degree of vascularity, (5) patient age (between 35 and 65 years), and (6) availability of clinical patient data. Frozen tissue samples embedded in OCT were cut at −21 °C into 8 μm serial sections using a cryotome (Leica CM1900, Richmond Hill, ON, Canada). Sections were mounted on Superfrost Plus microscope slides (Fisher Scientific, Ottawa, ON, Canada) and kept at −80 °C until use. This study was approved by the OTB and National Research Council Human Ethics Committees. All human subjects provided a written, informed consent.

Laser Capture Microdissection

To visualize blood vessels, tissue sections were fixed in 75% ethanol, washed with water, and incubated for 3 min at RT with fluorescein-conjugated Ulex Europaeus Agglutinin I (UEA1, Vector Laboratories) diluted (1:20 or 1:100) in D-PBS (Wisent, Inc., St-Jean Baptiste, QC, Canada). The slide was washed in D-PBS (30 s), dehydrated in 75, 95, and 100% ethanol (30 s), delipidated in xylene (5 min), and air-dried. Blood vessels were captured on CapSure Macro LCM Caps (Molecular Devices, Downingtown, PA) using an Arcturus PixCellII Laser Capture Microdisection System with fluorescence viewing option. The microdissection laser was set to 7.5 μm spot size and 850 μs pulse duration. The power was adjusted to the lowest value possible to allow efficient capture (between 30 and 70 mW). For each patient, a total of 6000−10 000 shots from both nonmalignant and tumor tissue sections were captured on 3 to 6 caps. Caps were stored at −80 °C until use.

Tryptic Digestion and Mass Spectrometry

Trypsin digestion was performed by placing between 25 and 30 μL of digestion solution (20 μg/mL trypsin in 50 mM ammonium bicarbonate/15% acetonitrile) per 1000 LCM shots directly on the cap membrane and incubating overnight at 37 °C. Pooled tryptic digests were analyzed by nanoLC−ESI−MS (20−40 μL per run). Quantification runs were performed on a Q-TOF Ultima mass spectrometer coupled to a NanoAcquity UPLC system (Waters, Milford, MA). Samples were loaded on a NanoAcquity symmetry C18 trap (Waters) and separated on a 10 cm × 100 μm I.D. C18 column (Waters, 1.7 μm BEH130C18) at ∼250 nL/minute using a 68 min gradient: 0−45% solution B (100% ACN/0.1% formic acid) over 66 min and 45−95% B over 2 min. Ten minute washes in 40% B were followed by 20 min blank gradients between each sample to minimize carryover effects. Continuum MS spectra were acquired in the TOF-MS mode between m/z 400−2000 with an acquisition duration of 1 s. Under these conditions, the average peptide elutes over a time period of ∼20 s, allowing 15−20 spectra to be collected over the chromatographic peak. For technical replicates, the entire set of nonmalignant and tumor digests was analyzed using these same parameters three times on separate days. The volume of tryptic digest loaded in the second and third technical replicates was adjusted to even out sample loading based on the median intensity values of multiply charged ions (excluding keratin and trypsin ions present in a mock digest) in the first technical replicate.

Both automated and targeted nano-LC−ESI−MS/MS were used for peptide identification. For the targeted analysis, peptides showing a visual change in expression between nonmalignant and tumor samples using MSight[23] were sequenced by MS/MS on the Q-TOF Ultima using an include list with a specified mass, charge, and time window, under identical chromatographic conditions as the quantification runs. MS/MS was set to trigger exclusively on ions contained in the include list with the following parameters: 3 MS/MS per scan, exclude after MS/MS for 10 s, survey intensity threshold = 15, peak detection window = 2.5 Da. The automated MS/MS analysis was performed on an LTQ-Orbitrap-XL mass spectrometer (Thermo) under similar chromatographic conditions with an MS scan at 60k resolution in the FTMS analyzer and data-dependent turbo MS/MS scans on the top 3 ions in the trap with dynamic exclusion (180 s). Peptides identified by both methods were manually aligned with the Q-TOF quantification runs using MSight, as previously described.[24]

Database Searches

All MS/MS spectra were assigned to peptide sequences using Mascot v2.2. For Q-TOF data, peaklists were generated using PeptideAuto within MassLynx 4.1 using these parameters:

smooth (window = 4, # = 2, mode = Savitzky Golay), centroid (min peak width at half height = 4, centroid top = 80%). The resulting peak lists were searched against the *Homo sapiens* Swissprot database (sprot_57.14, 20345 sequences; parameters: enzyme = trypsin; modifications = carbamidomethyl (C, fixed), oxidation (M, variable); peptide tolerance = 1.2 Da; fragment tolerance = 1.2 Da; 1 missed cleavage allowed). Decoy database searches were used to estimate the false positive identification rate at different Mascot scores as follows (Mascot score >50 = 1.1%; > 45 = 2.9%; > 40 = 8.9%). In addition, all Q-TOF peptide identifications were manually verified. No cysteine containing peptides were present in our final list, as expected based on our search parameters and our sample preparation protocol that eliminated reduction/alkylation.

Orbitrap data was converted to mzXML using Msconvert from the ProteoWizard version 2.0.1905 package (http://proteowizard.sourceforge.net/index.html) with the following parameters: −mzXML −32 −filter 'peakPicking true [2,3]'. MGF files were then generated from the mzXML file using MzXML2Search from the Trans Proteomics Pipeline project (TPP-4.3.1, http://tools.proteomecenter.org/wiki/index.php?title=Software:TPP) and searched against the *Homo sapiens* Swiss-Prot database (sprot_57.8, 20401 sequences) using the same parameters described above. Search results were subsequently filtered to remove peptides with a delta mass >15 ppm or a score <40. Under these conditions, the false positive identification rate based on decoy database searches was 1.1%. Peptides with a score >50 had a false positive rate of ∼0.3%.

Quantification by LC−MS and Statistical Analysis

Peptides identified by either the targeted or automated analysis were quantified using in house software, based on MatchRx.[25] For quantification, the mass of centroided ions within the Q-TOF quantitation MS runs was required to be within 40 ppm of the theoretical peptide mass. Within each patient, the peptide intensities between nonmalignant and tumor were normalized so that the median intensity of all multiply charged ions quantified in every MS runs was equal, after excluding ions identified as trypsin or keratin. Peptides present in multiple proteins were assigned to the protein with the most peptides identified. If two or more proteins match all assigned peptides, these accession numbers are listed in the table as an alternate identification. Protein intensities from each MS run were calculated by summing the intensities of all unique peptides derived from that protein. When calculating fold change between nonmalignant and tumor samples, proteins with intensity values only in tumor (i.e., not in nonmalignant) or only in nonmalignant were assigned a fold change of 8 ($\log_2$ ratio of 3) or −8 ($\log_2$ ratio of −3.0), respectively. To identify differentially expressed proteins, two statistical tests were employed for each protein, one to compare data from all nonmalignant tissues to all tumor tissues and another to look at the expression of each protein within a single patient. First, the average normalized intensity values for the 6 adjacent nonmalignant samples were compared to the average normalized intensity values for the 6 tumor samples using a paired two-tailed student *t* test in Microsoft Excel. Proteins were considered differentially expressed if $p < 0.05$ and the average fold-change between nonmalignant and tumor was >2. Second, to identify proteins that may be expressed in only a subset of tumors, individual paired *t* tests were performed for each patient by comparing the intensity values of the 3 technical repeats from nonmalignant and tumor using a paired student *t* test. If 2 or more patients (out of 6) had $p < 0.05$ and a fold-change >2, then this protein was also considered differentially expressed, regardless of the protein expression in the other samples (equivalent to $p < 0.05$, assuming a binomial distribution for a series of independent Bernoulli trials).

Immunofluorescence

Breast tissue sections were incubated in methanol for 10 min at RT, rinsed with 0.2 M PBS (pH 7.3)/0.1% Triton-X, and incubated in a universal blocking solution (Dako Diagnostic, Mississauga, ON, Canada) for 1 h at RT followed by incubation with a polyclonal sheep antihuman CD31 antibody (1:20; R&D System, Minneapolis, MN) for 1.5 h at RT or overnight at 4 °C. Sections were then washed with PBS and incubated with the secondary antibody, Alexa Fluor 488-labeled antisheep IgG (1:600; Molecular Probes, Eugene, OR) or Alexa Fluor 568-labeled antisheep IgG (1:800; Molecular Probes, Eugene, OR) for 1 h at RT. Slides were washed with PBS and counterstained with a mouse antihuman IQGAP1 (1:100; BD Transduction Laboratories), rabbit antihuman SERPINH1 (1:25; LifeSpan Biosciences), rabbit antihuman TAGLN2 (1:25; ProteinTech Group, Chicago, IL), rabbit antihuman CLIC1 (1:50; LifeSpan Biosciences), goat antihuman BGN (1:150; R&D System, Minneapolis, MN), antimouse LCP1 (1:250; Abcam), mouse antihuman THBS1 (1:50; LifeSpan Biosciences), rabbit antimouse HSP90AB1 (1:25; LifeSpan Biosciences) and/or mouse antihuman α-smooth muscle actin antibodies (1:100; R&D System, Minneapolis, MN) for 1.5 h at RT followed by incubation with their respective secondary antibodies (Alexa Fluor antirabbit, antimouse or antigoat) for 1 h at RT after washing with PBS. Sections were then rinsed with milli-Q water and dehydrated by sequential exposure to 70, 96 and 100% ethanol (30 s each) followed by a 5-min treatment with xylene (Anachemia, Montreal, QC, Canada). Sections were air-dried, rinsed in xylene, hydrated with decreasing concentrations of ethanol (100%, 96%, 70%, 30 s each) and coverslipped with Fluorescent mounting media (Dako Diagnostic, Mississauga, ON, Canada) spiked with 5 μg/mL of Hoechst33342 (Molecular Probes, Eugene, OR).

Western Blot Analysis

Breast tissue sections were fixed and delipidated as described above for the lectin staining prior to LCM, but excluding the lectin. Proteins were extracted from the entire section by incubation with 150 μL of 1× NuPage LDS sample buffer (Invitrogen) on ice for 20 min. Protein extracts were sonicated, centrifuged at 15 000× *g* for 20 min to remove cellular debris, and quantified using the Bio-Rad DC Protein assay. Equal quantities of total protein were reduced using 50 mM DTT (Sigma), separated by SDS-PAGE, and transferred to PVDF membranes using standard protocols. Membranes were blocked with 5% milk in TBS-T (10 mM Tris, 150 mM NaCl, 0.5% Tween 20, pH 8.0), incubated with primary antibody, washed with TBS-T, incubated with HRP-labeled secondary antibody, and developed using ECL Plus Western Blotting Detection System (Amersham). The primary antibodies and dilutions used were: anti-TAGLN2 (Proteintech Group, 1:500), anti-L-plastin (Abcam, 1:1000), anti-SERPINH1 (MJS Biolynx, 1:67), anti-ARPC3 (Novus Biologicals, 1:100), and anti-ATP5B (3D5, Santa Cruz, 1:200).

Microarray Data and Survival Curve Analysis

Gene expression profiles and patient survival data for breast cancer data sets including data from 236, 295, and 286 patients

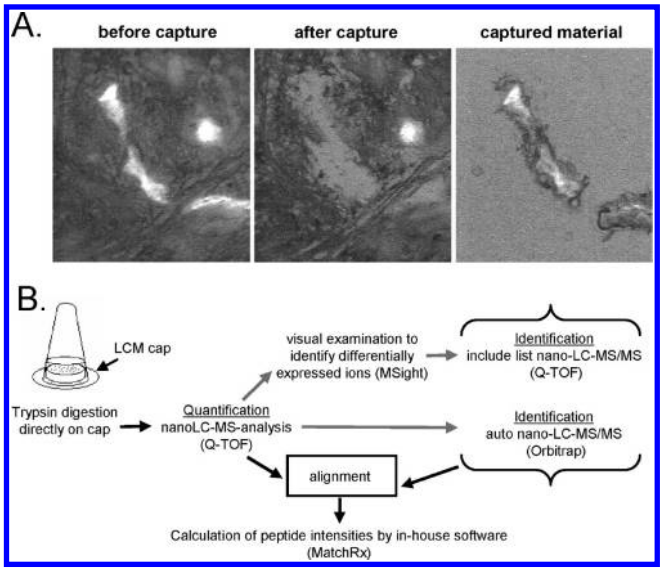

Figure 1. Laser capture microdissection (LCM) of microvessels from clinical breast tumors and analysis of extracted proteins using a label-free mass spectrometry based method. (A) Example of a laser captured microvessel from an IDC tumor section is shown. The intact tissue before capture shows a highlighted microvessel after labeling with fluorescein-conjugated UEA1. After capture of the microvessel, the highlighted vessel has been lifted from the tumor section and placed on the LCM cap ("captured material"). (B) Brief workflow showing the steps used to analyze proteins in the captured microvessels.

were obtained from Miller et al.,[26] Chang et al.,[27] and Wang et al.,[28] respectively. To evaluate the prognostic value of a set of genes based on the gene expression profiles and associated survival information of the tumor samples, we performed a Kaplan−Meier analysis by implementing the Cox−Mantel log-rank test using R, a statistical computing language (http://www.r-project.org/), as described previously.[29,30]

RESULTS AND DISCUSSION

Isolation of Microvessels from IDC and Adjacent Nonmalignant Tissue by Laser Capture Microdissection

To search for vascular markers of invasive ductal carcinoma (IDC), we used laser capture microdissection (LCM) to enrich for blood vessels in patient-matched samples of IDC and adjacent nonmalignant tissue. Ten matched pairs were acquired through the Ontario Tumour Bank. However, due to particularly low levels of vascularization in 3 patient samples, vessels were only captured for 7 matched pairs. Clinical information, including pathological classification, for these 7 patients is provided in Supplementary Table 1 (Supporting Information). Microvessels were identified using fluorescein-labeled Ulex Europaeus Agglutinin I (UEA1), a lectin that specifically binds to fucose residues of glycoproteins or glycolipids on endothelial cells.[31,32] Since UEA1 occasionally recognizes cells of epithelial origin as well, only labeled areas that had the characteristic morphology of vessels were captured. An example of an excised microvessel is shown in Figure 1A. In order to capture a comparable number of vascular cells from the nonmalignant and IDC tumor samples, the same number of laser shots was used for each patient-matched sample set. As expected, the IDC tumor samples were more highly vascularized and contained less fat deposits than the adjacent nonmalignant tissue.

Identification of Differentially Expressed Proteins in Microvessel-Enriched Fractions from IDC and Adjacent Nonmalignant Clinical Tissues

Proteins in the microdissected vessels were digested using a simplified protocol where trypsin solution containing 15% acetonitrile was incubated directly on the laser-captured microvessels (see Figure 1B). When compared to more traditional sample preparation methods involving separate steps for solubilization and enzymatic digestion, this on-cap digestion method minimizes sample manipulation, lessens sample loss, and reduces keratin contamination. Similar to direct digestion in methanol solutions,[33,34] the use of this procedure also appears to enrich for extracellular and cell surface proteins relative to the very abundant, but less accessible, cytoskeletal proteins.

For quantification, each digest was analyzed three separate times by nanoLC−MS on a Q-TOF instrument and the resulting peptide ions were quantified using a label-free method based on the number of ion counts under the LC−MS peak. A mock digest without any captured tissue was also analyzed to enable the identification of contaminant ions originating from trypsin autocleavages and keratins. Initially, visual examination of the LC−MS data was used to determine multiply charged ions that were differentially expressed between IDC and adjacent nonmalignant vessels. These ions of interest were then targeted for identification by MS/MS in subsequent runs using an include list. In addition, a limited number of samples were analyzed by automated LC−MS/MS on a LTQ-Orbitrap instrument. These two MS/MS methods, followed by database searching using Mascot, resulted in the identification of 560 unique peptides, which could be assigned to 182 unique proteins. Of these proteins, 94 were identified by more than one peptide, while 88 were identified by a single peptide. Despite the low number of peptides identified for each protein, the false positive identification rate of the 182 identified proteins was estimated at only 1% using a decoy database search strategy. The peptide sequences identified for each protein, including m/z, z, Mascot scores, retention time, and delta mass values, are provided in Supplementary Table 2 (Supporting Information). The intensity values for each individual peptide, as well as summed intensity values for each protein, are also provided. The quantitative data was quite consistent between the three technical repeats; protein intensities had a median relative standard deviation of 18% with an interquartile range of 10−31%. Also, individual peptides belonging to the same protein generally showed similar expression patterns, with a median Pearson coefficient of correlation of 0.88 (quartile range: 0.68−0.96) for the average intensity values of the 14 samples (7 IDC tumor and 7 nonmalignant).

To visualize the protein expression data across individual patients, we generated a heat map of the $\log_2$ ratio of protein intensity in the IDC tumor microvessel fractions relative to the nonmalignant tissue in each patient (Figure 2). In general, five of the seven patients showed similar patterns of expression, while two patients, A00299 and A00319, were quite different. These differences may reflect natural heterogeneity between individual tumors or they may result from other issues, such as misclassification of adjacent nonmalignant tissue or differences in tumor collection. In fact, during LCM capture, we noted that the nonmalignant and tumor samples from patient A00299 looked quite similar to each other. In this patient, both the nonmalignant and tumor sections looked more phenotypically "normal" — both had relatively low levels of vascularization and significant fat deposits. Based on the noted discrepancy in phenotype and the

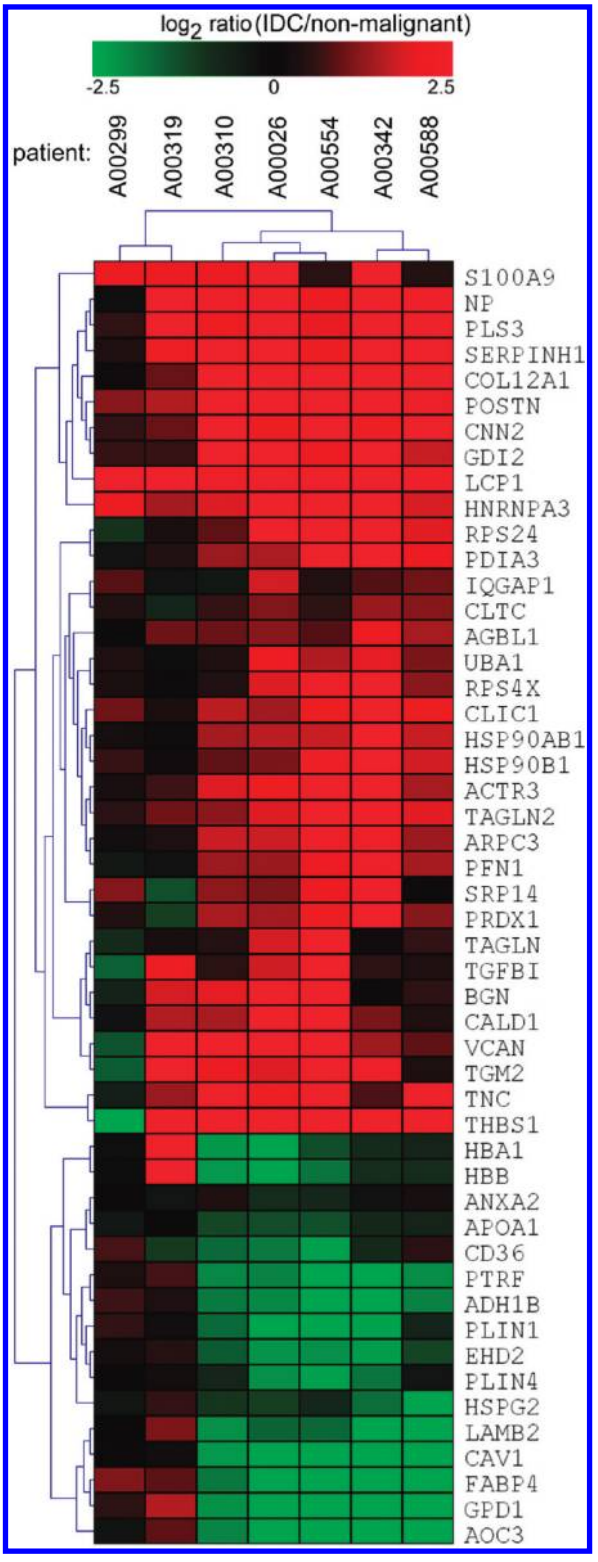

Figure 2. Differentially expressed proteins identified from microvessels isolated from patient-matched IDC tumors and adjacent nonmalignant tissue. A heat map showing the $\log_2$ ratio of 50 differentially expressed proteins in each of the 7 individual patients was produced using MeV v4.5.[61] Proteins that showed higher protein expression in tumor vessels than in vessels from adjacent nonmalignant tissue are displayed in red and lower expression is displayed in green. Samples and proteins were organized by hierarchical clustering using average linkage and Euclidean distance. The proteins are identified by their gene symbol as found in the Uniprot database.

quantitative MS results, we have excluded patient A00299 from our statistical analysis. As can be seen in Figure 2, the correlation between the other 5 patients is quite strong, especially considering the different clinical characteristics of the IDC tumors (see Supplementary Table 1, Supporting Information). We believe that the design of our experiments, using patient-matched tissues and an enriched cell population, may contribute to this correlation.

Statistical analysis based on paired student *t* tests identified 126 proteins that were differentially expressed between microvessels isolated from IDC and from nonmalignant tissues. Of these, 86 proteins were more highly expressed in the tumor vessels and 40 were more highly expressed in the nonmalignant vessels. These two groups of proteins are listed in Tables 1 and 2, respectively. Proteins that were highly expressed in tumor vessels fell into several major functional categories, including RNA-binding proteins, regulators of the actin cytoskeleton, extracellular matrix (ECM) proteins, protein chaperones, metabolic enzymes, signal transduction molecules, and regulators of vesicular trafficking. The proteins that are under-expressed in tumor vessels include metabolic enzymes and ECM proteins, but also contain a number of proteins involved in lipid and fatty acid metabolism, major blood proteins, and proteins involved in caveolae formation. The relatively high proportion of identified proteins that were differentially expressed reflects the experimental design, particularly the include-list guided MS/MS, which biased protein identification to peptides with an apparent change in abundance between IDC and nonmalignant samples.

Evaluation of Selected Proteins by Immunofluorescence and Western Blotting

Eight proteins that were identified as overexpressed in IDC vessels were selected for further validation by fluorescent immunohistochemistry (IHC) of the adjacent nonmalignant and IDC tissue sections. Since secreted and cell surface proteins make particularly promising targets for cancer diagnosis and therapy, we focused our IHC efforts on this subset of proteins. To determine expression levels in the vasculature, tissue sections from at least 3 different patients were fluorescently stained for the antigen of interest (in red), nuclei (Hoechst stain, in blue), and CD31 (in green), a marker of endothelial cells in blood vessels (Figure 3). In both the nonmalignant and IDC tissue sections, seven of the eight proteins were expressed in all or some microvessels, as demonstrated by colocalization with CD31. Although the remaining protein, L-plastin (LCP1), did not show significant staining of the CD31-positive endothelial cells themselves, it was significantly up-regulated in perivascular cells surrounding the vessels (see Figure 3D), likely explaining the presence of this protein in our microdissected samples.

In addition to expression associated with the vasculature, several proteins that we examined by IHC were also expressed in the mammary gland ducts, namely Transgelin 2, HSP90AB1, IQGAP1, and Clic-1. It is possible that these proteins are up-regulated in the endothelial and pericytes/smooth muscle cells of the tumor vessels. However, since tumor cells are known to infiltrate into the vasculature, it is also possible that tumor cells originating from the ducts were captured by our LCM method. Thus, some of the proteins identified in our experiments may reflect increased expression in tumor cells, rather than exclusive markers of tumor vasculature. For example, IQGAP1 showed widespread expression in the tumor, but with very limited expression in the nonmalignant tissue. This finding is consistent

Table 1. Proteins over-Expressed in Laser-Captured IDC Tumor Microvessels

overexpressed in IDC					fold change (tumor/nonmalignant)	
acc[a]	symbol[b]	protein name[b]	# unique peptides	max Mascot score	mean[c]	median[c]
		Cytoskeletal proteins				
O15145	ARPC3	Actin-related protein 2/3 complex subunit 3	1	61	3.16	3.26
P61158	ACTR3	Actin-related protein 3	1	51	4.13	4.18
P07737	PFN1	Profilin-1	2	77	2.64	2.63
P13797	PLS3	Plastin-3	3	73	6.84	6.87
P13796	LCP1	Plastin-2	1	72	6.46	6.22
Q01995	TAGLN	Transgelin	6	100	2.04	1.45
P37802	TAGLN2	Transgelin-2	5	140	3.62	3.74
P12814	ACTN1	Alpha-actinin-1	11	105	1.81	1.80
O43707	ACTN4	Alpha-actinin-4	1	88	1.79	1.75
P60660	MYL6	Myosin light polypeptide 6	2	61	1.81	1.88
P35579	MYH9	Myosin-9	18	125	2.49	2.62
O14950 [P19105]	MYL12B	Myosin regulatory light chain 12B	2	64	1.87	1.66
Q05682	CALD1	Caldesmon	1	108	3.67	2.80
Q99439	CNN2	Calponin-2	1	62	4.90	5.69
Q9BQE3 [P68363, Q71U36]	TUBA1C	Tubulin alpha-1C chain	8	113	2.23	2.00
P07437	TUBB	Tubulin beta chain	9	152	2.37	2.33
		Extracellular Matrix				
P02751	FN1	Fibronectin	24	137	7.81	7.96
P21333	FLNA	Filamin-A	16	126	2.06	1.62
Q15063	POSTN	Periostin	15	109	6.81	7.17
Q99715	COL12A1	Collagen alpha-1(XII) chain	10	85	7.31	8.88
P24821	TNC	Tenascin	6	82	5.62	5.90
P46940	IQGAP1	Ras GTPase-activating-like protein IQGAP1	3	115	1.48	1.55
P05109	S100A8	Protein S100-A8	1	42	5.76	8.00
P06702	S100A9	Protein S100-A9	3	95	4.06	4.17
P21810	BGN	Biglycan	3	79	3.34	3.64
P13611	VCAN	Versican core protein	3	67	6.18	7.12
P27797	CALR	Calreticulin	2	51	2.86	3.07
O00299	CLIC1	Chloride intracellular channel protein 1	1	92	3.62	3.70
P07996	THBS1	Thrombospondin-1	1	46	8.42	8.00
Q15582	TGFBI	Transforming growth factor-beta-induced protein ig-h3	1	52	2.55	2.2
		Other				
Q06830	PRDX1	Peroxiredoxin-1	1	51	2.52	2.71
P21980	TGM2	Protein-glutamine gamma-glutamyltransferase 2	1	47	4.11	4.89
Q96MI9	AGBL1	Cytosolic carboxypeptidase 4	1	45	2.37	2.14
P22314	UBA1	Ubiquitin-like modifier-activating enzyme 1	2	70	2.22	2.45
		Protein folding/chaperone function				
P30101	PDIA3	Protein disulfide-isomerase A3	2	65	4.16	3.39
P07237	P4HB	Protein disulfide-isomerase	1	47	3.58	4.13
P50454	SERPINH1	Serpin H1	7	69	7.54	6.23
P07900	HSP90AA1	Heat shock protein HSP 90-alpha	1	60	2.55	2.99
P08238	HSP90AB1	Heat shock protein HSP 90-beta	7	91	2.96	3.09
P14625	HSP90B1	Endoplasmin	4	71	2.83	2.70
P04792	HSPB1	Heat shock protein beta-1	2	78	1.48	1.25
P11021	HSPA5	78 kDa glucose-regulated protein	1	64	2.78	3.00

dx.doi.org/10.1021/pr101267k |J. Proteome Res. 2011, 10, 2479–2493

Table 1. Continued

overexpressed in IDC					fold change (tumor/nonmalignant)	
acc[a]	symbol[b]	protein name[b]	# unique peptides	max Mascot score	mean[c]	median[c]
		Metabolic enzymes				
P04075	ALDOA	Fructose-bisphosphate aldolase A	2	143	1.37	1.66
P04406	GAPDH	Glyceraldehyde-3-phosphate dehydrogenase	3	76	2.92	2.89
P00338	LDHA	L-lactate dehydrogenase A chain	3	54	2.02	1.98
P07195	LDHB	L-lactate dehydrogenase B chain	1	66	1.13	0.84
P00491	NP	Purine nucleoside phosphorylase	1	42	6.82	6.53
P14618	PKM2	Pyruvate kinase isozymes M1/M2	5	134	3.05	3.88
		Mitochondrial transport				
P12236	SLC25A6	ADP/ATP translocase 3	2	62	2.09	2.48
P21796	VDAC1	Voltage-dependent anion-selective channel protein 1	3	136	1.91	2.46
		N-glycosylation				
P39656	DDOST	Dolichyl-diphosphooligosaccharide--protein glycosyltransferase 48 kDa subunit	1	60	2.40	2.60
P04843	RPN1	Dolichyl-diphosphooligosaccharide--protein glycosyltransferase subunit 1	1	48	2.14	2.41
		RNA binding proteins and regulators of protein translation				
P60842 [Q14240]	EIF4A1	Eukaryotic initiation factor 4A-I	2	72	2.52	2.70
Q13838 [O00148]	BAT1	Spliceosome RNA helicase BAT1	1	43	2.75	2.87
P37108	SRP14	Signal recognition particle 14 kDa protein	1	54	1.90	2.26
Q12905	ILF2	Interleukin enhancer-binding factor 2	1	30	2.12	2.48
P68104 [Q5VTE0]	EEF1A1	Elongation factor 1-alpha 1	4	64	2.79	3.01
P24534	EEF1B2	Elongation factor 1-beta	1	103	5.50	6.04
P29692	EEF1D	Elongation factor 1-delta	1	57	2.28	2.78
P26641	EEF1G	Elongation factor 1-gamma	2	55	2.91	2.78
P13639	EEF2	Elongation factor 2	1	66	4.16	4.88
P51991	HNRNPA3	Heterogeneous nuclear ribonucleoprotein A3	2	69	7.89	4.71
Q14103	HNRNPD	Heterogeneous nuclear ribonucleoprotein D0	1	59	2.32	2.83
P55795 [P31943]	HNRNPH2	Heterogeneous nuclear ribonucleoprotein H2	1	43	2.23	2.29
P61978	HNRNPK	Heterogeneous nuclear ribonucleoprotein K	2	89	2.37	2.72
P52272	HNRNPM	Heterogeneous nuclear ribonucleoprotein M	1	58	2.17	2.58
O60506	SYNCRIP	Heterogeneous nuclear ribonucleoprotein Q	1	47	6.08	6.85
Q00839	HNRNPU	Heterogeneous nuclear ribonucleoprotein U	1	116	1.70	2.05
P26599	PTBP1	Polypyrimidine tract-binding protein 1	1	53	2.43	2.89
P62701	RPS4X	40S ribosomal protein S4, X isoform	1	48	2.68	2.91
P62753	RPS6	40S ribosomal protein S6	1	112	3.73	3.46
P62081	RPS7	40S ribosomal protein S7	1	57	3.03	3.28
P62244	RPS15A	40S ribosomal protein S15a	1	57	4.34	4.91
P62847	RPS24	40S ribosomal protein S24	1	67	3.64	4.66
P39023	RPL3	60S ribosomal protein L3	1	51	2.83	3.54
P61313	RPL15	60S ribosomal protein L15	1	45	2.41	2.62
Q07020	RPL18	60S ribosomal protein L18	1	93	2.08	1.85
P84098	RPL19	60S ribosomal protein L19	1	104	2.49	2.47
		Signal transduction				
P63104	YWHAZ	14-3-3 protein zeta/delta	1	136	2.30	2.21
P27348	YWHAQ	14-3-3 protein theta	1	85	3.13	3.96
P06748	NPM1	Nucleophosmin	1	77	2.21	2.92
P42224	STAT1	Signal transducer and activator of transcription 1-alpha/beta	1	34	2.89	2.48

dx.doi.org/10.1021/pr101267k |J. Proteome Res. 2011, 10, 2479–2493

Table 1. Continued

overexpressed in IDC					fold change (tumor/nonmalignant)	
acc[a]	symbol[b]	protein name[b]	# unique peptides	max Mascot score	mean[c]	median[c]
		Vesicular trafficking				
Q00610	CLTC	Clathrin heavy chain 1	4	97	1.62	1.86
P55072	VCP	Transitional endoplasmic reticulum ATPase	2	73	1.58	1.47
P50395	GDI2	Rab GDP dissociation inhibitor beta	1	46	4.62	5.18
P49755	TMED10	Transmembrane emp24 domain-containing protein 10	1	75	2.74	3.53

[a] Swiss-Prot accession number (additional accession numbers containing the same set of peptides are listed in brackets when applicable). [b] Underlined proteins belong to the 29-protein set used in the survival analysis. [c] Mean and median fold change of the 6 patient samples.

with several previous studies that showed a strong up-regulation of IQGAP1 in a number of different cancers, including breast cancer (reviewed in Johnson et al.[35]).

Several proteins, such as Biglycan, Serpin H1, Transgelin 2, and Clic-1 showed expression in both the CD31-positive endothelial cells and in perivascular cells surrounding the vessels. To identify the nature of these perivascular cells, the tissue sections were stained with antibodies against smooth muscle actin (SMA), a marker of pericytes/smooth muscle cells (SMCs). Pericytes/SMCs are known to interact closely with endothelial cells and play an important role in regulating blood vessel maturation and blood flow. As shown in Figure 4, Biglycan, Serpin H1, and Transgelin 2 all colocalize with α-SMA in tumor tissues, suggesting that they are expressed in pericytes/SMCs. Although most tumor vessels were surrounded by a thick layer of SMA-positive cells, some vessels had a much smaller proportion of associated SMA-positive cells (see Figure 4C, right-most vessel). These may represent immature microvessels, which are often found in tumors.[36]

To further validate our proteomic results, we performed Western blotting using whole tissue protein extracts from the nonmalignant and IDC tumor samples from 2 different patients for which we had sample remaining after our previous analyses, patients A00026 and A00554. As can be seen in Figure 5, Serpin H1, Transgelin 2, Plastin-2/L-plastin, and ARPC3 are much more highly expressed in the tumor, confirming our mass spectrometry results which showed more than a 2.5 fold increase in the expression of these proteins. The bands for each of these three proteins are located at the expected molecular weight and show similar expression patterns for both patient samples. The anti-Transgelin-2 antibody recognized two distinct bands; the upper band is located at the predicted molecular weight of the intact protein (22 kDa), suggesting that the lower band may be a proteolytic cleavage product. Although the relative abundance of the two Transgelin-2 bands is different in the 2 patients analyzed, both bands are strongly up-regulated in the tumor samples of both patients. In contrast, ATP5B, a protein found to be similarly expressed in nonmalignant and IDC vessels in our mass spectrometry experiments, showed similar expression patterns in the nonmalignant and IDC tumor tissues.

Identification of a Prognostic Signature

To examine the potential prognostic power of the differentially expressed proteins identified in this study, we examined the correlation between the expression of these proteins and patient survival. Clinical information provided with the breast tumors analyzed in this study indicated that 2 of the 7 tumors used in our proteomic analysis were derived from patients who relapsed within 2 years of diagnosis (patient A00319: diagnosis 09/2005, deceased 06/2006 and patient A00342: diagnosis 10/2005, recurrence 2/2007). Since patients A00299 and A00319 did not correlate well with the others, these outlier samples were excluded from further analysis and we calculated the relative expression of each differentially expressed protein in the remaining "bad" outcome tumor (patient A00342) relative to the four "good" outcome tumors (patients A00310, A00026, A00554, and A00588). To do this, we first calculated the ratio (R1) of the expression of each protein in the IDC tumor tissue relative to the adjacent nonmalignant tissue for each patient. We then calculated the ratio (R2) of R1 of each protein for the "bad" outcome sample to the average R1 value of the 4 "good" outcome samples. Based on the data point distribution, we determined that if the R2 value of a protein was greater than 2.5 or less than 0.4, the protein appeared to be differentially modulated in "bad" and "good" tumors. A total of 29 proteins met these criteria; these proteins are underlined within Tables 1 and 2 and are also listed separately in Supplementary Table 3 (Supporting Information). Given the extremely low sample numbers, this analysis is by nature quite speculative; thus, we were interested in exploring the predictive power of this set of 29 proteins in a larger data set. Unfortunately, there are no publicly available data sets that include protein expression information linked to patient survival data. Therefore, we used three publicly available mRNA microarray data sets containing data from 236, 295, and 286 patient samples.[26−28] Despite the relatively low correlation between mRNA and protein levels, the mRNA expression values of the 29 genes identified through analysis of our proteomic data showed significant predictive power for breast cancer prognosis (Figure 6). This result suggests that the 29 protein set is a vascular prognostic signature that can be linked to patient outcome and also implies that at least some of these proteins may be involved in the regulation of specific tumor properties. The 29-protein set includes 17 proteins that were up-regulated in IDC tumors and 12 proteins were down-regulated. The up-regulated proteins include Biglycan, Clic-1, Serpin H1, and HSP90AB1 which were included in the immunohistochemistry analysis.

Differentially Expressed Proteins in IDC

Many proteins identified in this study have been previously associated with breast cancer, including Fibronectin, Periostin,[37] Tenascin C,[38] Versican,[39] and L-plastin.[40] Several proteins also have known roles in angiogenesis and endothelial cell biology,

Table 2. Proteins under-Expressed in Laser-Captured IDC Tumor Microvessels

underexpressed in IDC					fold change (tumor/nonmalignant)	
acc[a]	symbol[b]	protein name[b]	# unique peptides	max Mascot score	mean[c]	median[c]
		Lipid and fatty acid regulation and metabolism				
O60240	PLIN1	Perilipin-1	11	126	−3.54	−4.08
Q96Q06	PLIN4	Perilipin-4	8	105	−2.25	−2.37
P15090	FABP4	Fatty acid-binding protein, adipocyte	5	158	−8.79	−19.33
P33121	ACSL1	Long-chain-fatty-acid--CoA ligase 1	1	50	−4.66	−7.91
		Metabolic enzymes				
P21695	GPD1	Glycerol-3-phosphate dehydrogenase [NAD+], cytoplasmic	5	97	−7.16	−10.19
P00325	ADH1B	Alcohol dehydrogenase 1B	4	75	−3.92	−3.95
		Major blood proteins				
P02768	ALB	Serum albumin	9	84	−2.37	−2.33
P01842	IGLC1	Ig lambda chain C regions	1	61	−1.92	−2.09
P01859 [P01860]	IGHG2	Ig gamma-2 chain C region	1	78	−1.73	−1.88
P01861	IGHG4	Ig gamma-4 chain C region	1	78	−1.48	−2.44
P01877 [P01876]	IGHA2	Ig alpha-2 chain C region	2	92	−5.15	−3.96
P02647	APOA1	Apolipoprotein A-I	5	72	−1.84	−1.98
P69905	HBA1	Hemoglobin subunit alpha	3	95	−1.77	−2.09
P68871	HBB	Hemoglobin subunit beta	7	131	−1.99	−2.52
P02671	FGA	Fibrinogen alpha chain	2	77	−1.43	−2.32
P04275	VWF	von Willebrand factor	1	40	−1.78	−1.44
		Extracellular Matrix				
P02462	COL4A1	Collagen alpha-1(IV) chain	1	53	−2.10	−2.30
P08572	COL4A2	Collagen alpha-2(IV) chain	2	95	−1.78	−1.95
P12109	COL6A1	Collagen alpha-1(VI) chain	6	132	−1.25	−1.44
P12110	COL6A2	Collagen alpha-2(VI) chain	5	75	−1.41	−1.57
P12111	COL6A3	Collagen alpha-3(VI) chain	24	138	−1.33	−1.51
P55268	LAMB2	Laminin subunit beta-2	4	115	−4.41	−3.67
P11047	LAMC1	Laminin subunit gamma-1	3	104	−1.56	−1.71
P51888	PRELP	Prolargin	2	79	−1.42	−1.47
P98160	HSPG2	Basement membrane-specific heparan sulfate proteoglycan core protein	7	108	−2.11	−2.09
P55083	MFAP4	Microfibril-associated glycoprotein 4	1	63	−2.02	−1.64
Q9GZM7	TINAGL1	Tubulointerstitial nephritis antigen-like	1	48	−2.85	−2.68
		Caveolae				
Q03135	CAV1	Caveolin-1	2	76	−6.95	−8.83
O95810	SDPR	Serum deprivation-response protein	2	79	−3.59	−3.63
Q969G5	PRKCDBP	Protein kinase C delta-binding protein	1	48	−3.34	−3.68
		Cytoskeleton				
P17661	DES	Desmin	1	54	−3.94	−4.59
Q02413	DSG1	Desmoglein-1	1	73	−2.23	−2.22
Q9NZN4	EHD2	EH domain-containing protein 2	11	111	−2.75	−3.47
		Other				
P20774	OGN	Mimecan	1	91	−2.99	−2.05
P02511	CRYAB	Alpha-Crystallin B chain	1	73	−2.95	−5.33
P07305	H1F0	Histone H1.0	1	117	−2.40	−2.71
Q16853	AOC3	Membrane primary amine oxidase	4	90	−12.93	−15.96
Q5D862	FLG2	Filaggrin-2	1	50	−2.03	−2.89
Q6NZI2	PTRF	Polymerase I and transcript release factor	4	141	−3.61	−4.14
P16671	CD36	Platelet glycoprotein 4	2	104	−2.28	−2.55

[a] Swiss-Prot accession number (additional accession numbers containing the same set of peptides are listed in brackets when applicable). [b] Underlined proteins belong to the 29-protein set used in the survival analysis. [c] Mean and median fold change of the 6 patient samples.

dx.doi.org/10.1021/pr101267k |J. Proteome Res. 2011, 10, 2479–2493

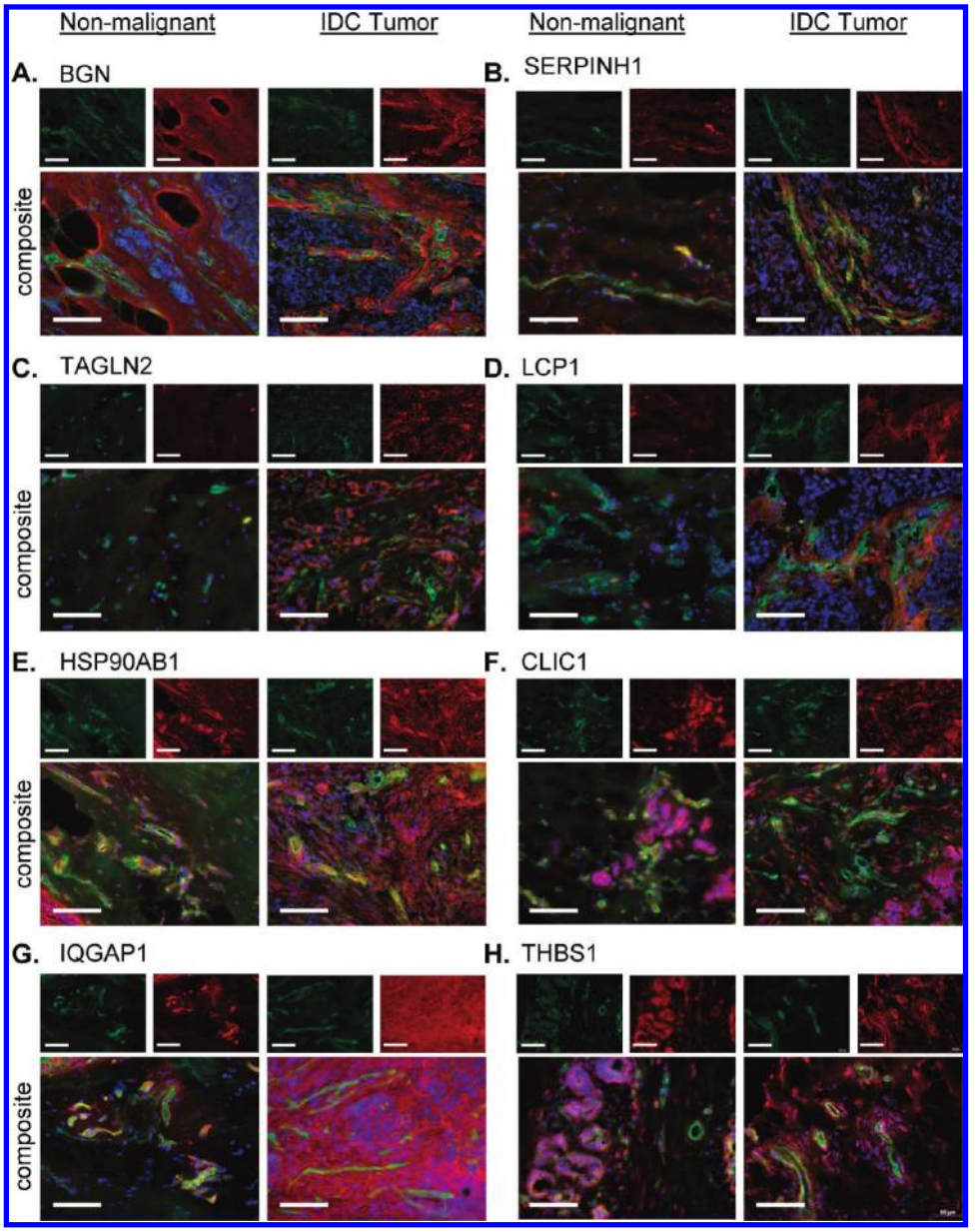

Figure 3. Immunohistochemistry analysis of selected proteins. Immunohistochemistry was used to determine the expression pattern of eight proteins that were identified in this study as overexpressed in IDC tumor vessels. Adjacent nonmalignant (left-hand panels) and IDC tumor (right-hand panels) tissue sections were labeled with the endothelial cell marker (anti-CD31, shown in green) and a protein of interest (shown in red). Composite images showing staining of CD31, the protein of interest, and DNA (Hoechst, blue) are shown below the smaller images showing individual staining. Proteins of interest in each panel are (A) Biglycan (BGN), (B) Serpin H1, (C) transgelin 2 (TAGLN2), (D) L-plastin (LCP1), (E) heat shock protein 90AB1 (HSP90-AB1), (F) Clic-1, (G) IQ-GAP1, and (H) Thrombospondin 1 (THBS1). Scale bars representing 100 μm are shown.

including Caldesmon,[41] Calponin-2,[42] Periostin, and Tenascin C. In the following sections, we will discuss several of the differentially expressed proteins identified in these experiments in the context of cancer biology and tumor angiogenesis.

A. Extracellular Proteins. Our data suggests that the extracellular matrix associated with vessels undergoes a remodelling in IDC. For example, we see a consistent decrease in the expression of ECM proteins that comprise the vascular basement membrane, a thin layer of proteins surrounding the endothelial cells that serves to attach the vessel to the surrounding connective tissue. Protein components of the basement membrane include Collagen IV, Laminin, Perlecan/HSPG2, and Prolargin, all of which were underexpressed in tumor vessels. This likely reflects abnormalities in the basement membrane structure and composition in tumor vessels.[43] This hypothesis is supported by the lower level of abundant serum proteins (i.e., albumin, immunoglobulins, and hemoglobins) found in the IDC tumor vessels, suggesting lowered blood perfusion in tumor microvessels compared with nonmalignant microvessels. Interestingly, this abnormal basement membrane may serve to facilitate tumor cell metastasis by allowing tumor cells to enter the vasculature.

Other protein changes associated with the ECM include the up-regulation of Transforming growth factor beta-induced protein ig-h3 (Beta ig-h3) and Biglycan, and the down-regulation of

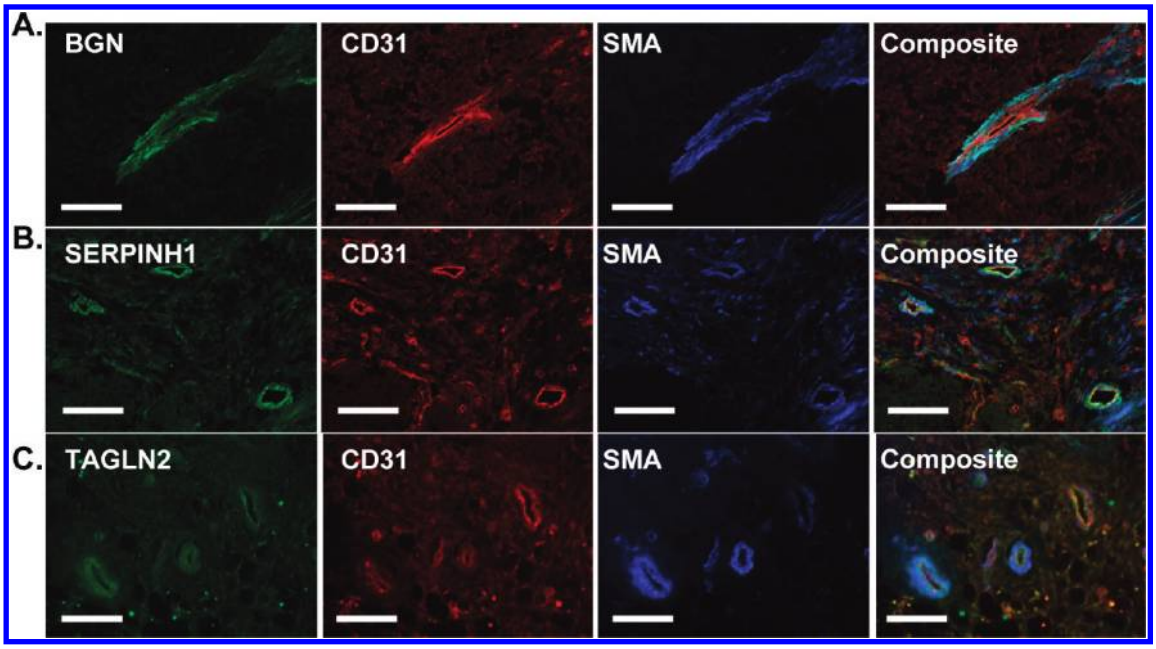

Figure 4. Biglycan (BGN), Serpin H1, and Transgelin-2 (TAGLN2) colocalize with smooth muscle actin (SMA), a marker of pericytes. Tissue sections from an IDC tumor were costained with antibodies against biglycan (A), Serpin H1 (B), or Transgelin-2 (C) (shown in green), anti-CD31 (red), and anti-SMA (blue). Staining of each individual marker is shown in addition to a composite image in the right-hand panel. Scale bars representing 100 μm are shown.

the three chains of Collagen VI. Interestingly, Beta ig-h3 protein has been shown to interact directly with Biglycan and Collagen VI forming a ternary complex and promoting collagen aggregation.[44] It is possible that the lower level of Collagen VI seen in our experiment may reflect a rearrangement of Collagen VI from a more soluble form in nonmalignant tissue, to a highly complexed, inaccessible form in tumor tissue. Serpin H1 may also play a role in remodelling the collagen fibers surrounding tumor vessels, since it has been shown to play a critical role in the proper folding and trafficking of collagen subunits.[45]

Thrombospondin 1 (THBS1), a protein that we identified as overexpressed in tumor vessels, is generally thought to negatively regulate tumorigenesis and angiogenesis.[46] However, several groups have reported an increase in THBS1 mRNA and protein in breast carcinomas. It has been suggested that the antiangiogenic effects of THBS1 must be overcome in order for cells to become tumorigenic; however, the mechanism of this change is not entirely understood. Interestingly, our results suggest that IDC tumor vessels have decreased expression of CD36, a cell-surface receptor that plays a significant role in mediating the antiangiogenic effect of THBS1. To our knowledge, a down-regulation of CD36 expression in tumor endothelial cells has not been proposed as a mechanism of THBS-1 resistance in tumors. Our data suggests that levels of CD36 may be a factor in this process.

Clic-1, a chloride channel, has not previously been reported as a marker of IDC or other breast carcinomas. However, recent proteomic studies have demonstrated that Clic-1 is overexpressed in other cancers that are associated with epithelial tissues, including gastric,[47] colorectal,[48] and nasopharyngeal[49] cancers. Our results suggest that Clic-1 is also expressed in the endothelial cells and pericytes/SMCs of the microvasculature in breast. In other cancers, the expression of Clic-1 has been shown to correlate with metastatic potential.[47,50] Furthermore, the genetic knockout of another Clic family member, Clic-4, leads to angiogenic defects in mice[51] and Clic-1 regulates endothelial cell growth and migration in culture,[52] suggesting the expression of Clic-1 in tumor vasculature seen in our proteomic and IHC studies may play a role in regulating tumor angiogenesis.

B. Cytoskeletal Proteins. Cell migration is a cyclical process that is largely driven by the polymerization and depolymerization of the actin cytoskeleton by a tightly regulated process that integrates cellular signals to drive reorganization of actin microfilaments in a concerted manner.[53,54] As might be expected, several of the cytoskeletal proteins found to be overexpressed in IDC vessels have been previously shown to be overexpressed in tumors by other groups. For example, IQGAP1 overexpression is linked to cell migration and invasion, at least partially through actin rearrangements mediated by the Arp2/3 complex. The expression of IQGAP in endothelial cells has also been linked to the regulation of angiogenesis.[55] The actinin proteins, Actinin-1 and Actinin-4, mediate the interaction between actin microfilaments with the cell membrane and, indirectly, to Collagen 12 alpha 1 in the extracellular matrix.[56] Other up-regulated proteins that regulate the actin cytoskeleton include myosin subunits that mediate contraction and cross-linking actin-binding proteins that bundle actin filaments, such as the Plastins, Calponin-2, and Filamin A.

More unexpectedly, a couple of cytoskeletal proteins that were found to be overexpressed in tumor vessels have been previously shown to be underexpressed in cancers. Profilin-1 has not only been shown to be downregulated in breast cancer tumors and cells, but also functions to negatively regulate cancer cell motility.[57,58] Similarly, Calponin-2 is downregulated in prostate cancer cells where it has been shown to inhibit proliferation and migration.[59] Presumably, the upregulation of Profilin-1 and Calponin-2 that we saw in this study is linked to higher expression of these proteins in IDC tumor vessels than nonmalignant

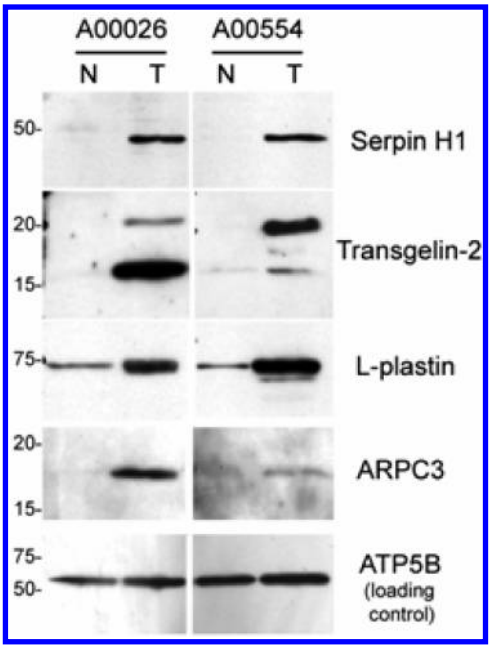

Figure 5. Evaluation of the expression of selected proteins in total protein extracted from two patient-matched IDC tumors and adjacent nonmalignant tissues by Western blot. Strong up-regulation of Serpin H1, Transgelin-2 (TAGLN2), L-plastin (LCP1), and Actin-related protein 2/3 complex subunit 3 (ARPC3) was seen in the IDC tumors from both patients. A Western blot against ATP5B, a protein that showed no difference in expression between tumor and adjacent nonmalignant tissues in our mass spectrometry data, was used as a loading control.

vessels. In fact, Calponin-2 has been recently shown to regulate vascular development, as demonstrated by defects in endothelial cell migration when Calponin-2 is knocked down in zebrafish embryos.[42] This suggests that Calponin-2 may positively regulate tumor angiogenesis, consistent with the higher expression observed in IDC tumors.

C. Translational Machinery and Protein Folding Proteins. A large number of up-regulated proteins identified in this study are RNA-binding proteins. These include several ribosomal proteins from the large 60S and small 40S subunits, as well as members of the ubiquitous heterogeneous nuclear ribonucleoprotein family, ILF2 (a subunit from the transcription factor, NFAT, that also binds RNA), the spliceosome RNA helicase BAT1, and eukaryotic translation initiation factor 4A-1. Several translation elongation factors were also up-regulated in tumor vessels. Interestingly, our data suggests that a large group of proteins, including these RNA binding proteins and elongation factors, as well as a number of heat shock proteins, appear to be coregulated. By comparing the protein intensities in the 7 nonmalignant and 7 IDC tumor samples, we found several groups of proteins that showed highly correlated expression patterns, as defined by a Pearson coefficient of correlation greater than 0.9 (data not shown). The largest group of coregulated proteins comprises the ribosomal proteins, elongation factors, RNA binding proteins, the heat shock proteins, and the N-glycosyltransferase subunits. The coregulation of these proteins involved in translation and protein folding suggests that protein expression is regulated at a post-transcriptional level. In fact, microarray data collected in parallel with this study revealed that many of the proteins that we observed to be strongly up-regulated did not have a corresponding change in their mRNA transcript levels (data not shown, manuscript in preparation).

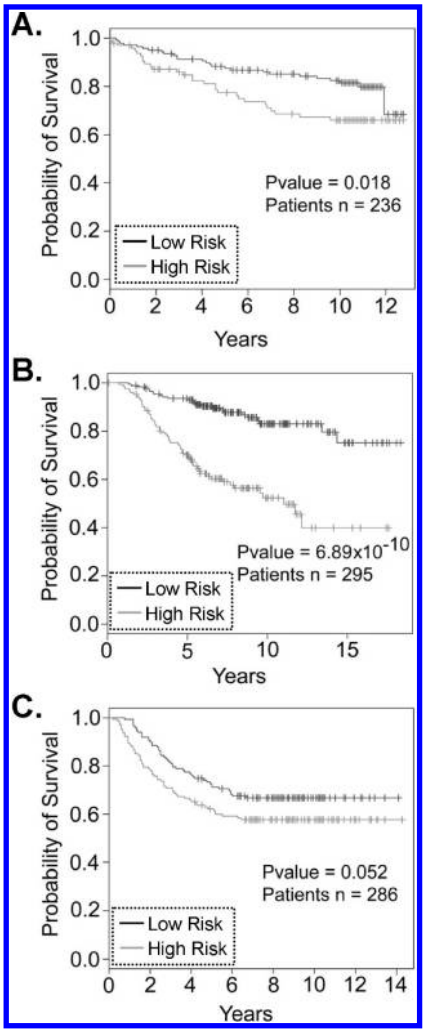

Figure 6. Survival curve analysis using a set of 29 proteins found to be differentially expressed between adjacent nonmalignant and IDC tumor vessels. Gene expression corresponding to the 29-protein set was used to categorize patients into high-risk or low-risk groups using three publicly available microarray studies from (A) Miller et al.,[25] (B) Chang et al.,[26] and (C) Wang et al.[27] containing data from 236, 295, and 286 patients respectively. The survival data corresponding to each group of patients in each data set is shown.

D. Proteins that May Be Derived from Nonvascular Cells. A number of proteins found to be more highly expressed in the nonmalignant samples are associated with the regulation or metabolism of lipids and fatty acids. These proteins include Perilipin-1 and 4, Fatty acid binding protein 4, and Long-chain fatty-acid-CoA ligase 1. As expected in breast tissue, the adjacent nonmalignant samples contained large areas of fat deposits, while the tumor samples were generally more "solid". Thus, it is possible that these proteins are derived from adipocyte cells that were located near blood vessels and thus were captured during the microdissection. As mentioned above, several major components of serum were also more highly expressed in nonmalignant vessels, likely reflecting decreased blood flow in tumor vessels.

E. Differentially Expressed Proteins in IDC: Proteins with Lesser-Known or Emerging Links to Breast Cancer. It is clear from the discussion above that a large number of

proteins that we found to be differentially expressed in microdissected vessels from IDC breast tumors and the adjacent nonmalignant tissue have been previously implicated in cancer progression and/or angiogenesis. This correlation with the published literature is reassuring and serves to validate the results found in this study. However, it is also interesting to note proteins that have not previously been strongly linked to cancer. These include proteins such as the carboxypeptidase AGBL1, the ADP/ATP translocase, Slc25A6, and the emp24 family member, TMED10. Roles in breast cancer are just emerging for other proteins. For example, a recent proteomics study identified Clic-1 as upregulated and Transgelin 2 as downregulated in a metastatic variant of a breast cancer cell line.[60] Other proteins mentioned above, such as beta Ig-h3, and Serpin H1, have been implicated in other types of cancer, but to our knowledge have not been previously linked to breast cancer. Our results suggest that these proteins may play an important role in the vasculature of invasive ductal carcinoma. However, further work will be required to determine the function of these proteins in the context of IDC progression and tumor angiogenesis.

CONCLUSIONS

Proteomic analysis of LCM isolated microvessels from IDC breast tumors and adjacent nonmalignant patient-matched tissues led to the identification of 126 differentially expressed proteins. The application of a survival curve analysis based on publically available microarray data sets highlighted several of these proteins as likely candidates for further follow-up functional experiments. For example, Serpin H1 was part of the 29-gene set that predicted patient survival and was shown by immunofluorescence to have an interesting expression pattern in perivascular cells, including pericytes/smooth muscle cells. However, given the imperfect correlation between mRNA and protein levels, we hypothesize that the survival curve analysis would be more highly predictive if we were able to use protein expression data rather than mRNA microarray data. As proteomic technologies advance to improve the depth and coverage in protein expression data sets, we anticipate that data from large numbers of well-characterized clinical samples will become available thereby facilitating this type of analysis. This will add yet another dimension to our understanding of the mechanisms that underlie breast tumor development.

ASSOCIATED CONTENT

Supporting Information

Supplementary Table 1: Clinical information for invasive ductal carcinoma samples. Supplementary Table 2: Mass spectrometry data for all identified proteins, including protein and peptide intensities in individual MS runs and individual patients and peptide identification details. Supplementary Table 3: Members of the 29 gene/protein set utilized in the survival curve analysis. This material is available free of charge via the Internet at http://pubs.acs.org.

AUTHOR INFORMATION

Corresponding Author

*Jennifer J. Hill, Institute for Biological Sciences, National Research Council Canada, 100 Sussex Drive, Rm 2038, Ottawa, ON K1A 0R6, Canada. E-mail: Jennifer.Hill@nrc-cnrc.gc.ca. Phone: (613) 993-7206. Fax: (613) 952-9052.

ACKNOWLEDGMENT

We would like to thank Dr. Arsalan Haqqani for help with the data normalization, Dr. Phuong Le for tissue embedding, sectioning, and advice on the LCM, Christiane Cantin for tissue sectioning, Luc Tessier for LC-MS support, and Wen Ding for helpful discussions on sample handling. This work was supported with funds from Phases III and IV of the Cancer Program as part of the Genomics and Health Initiative of the government of Canada.

REFERENCES

(1) Boyle, P.; Levin, B. *The International Agency for Research on Cancer-World Cancer Report 2008*; WHO Press: Geneva, Switzerland, 2008.

(2) Fox, S. B.; Generali, D. G.; Harris, A. L. Breast tumour angiogenesis. *Breast Cancer Res.* **2007**, *9* (6), 216.

(3) Greenberg, S.; Rugo, H. S. Triple-negative breast cancer: role of antiangiogenic agents. *Cancer J.* **2007**, *16* (1), 33–8.

(4) Le Bourhis, X.; Romon, R.; Hondermarck, H. Role of endothelial progenitor cells in breast cancer angiogenesis: from fundamental research to clinical ramifications. *Breast Cancer Res. Treat.* **2010**, *120* (1), 17–24.

(5) Gordon, M. S.; Mendelson, D. S.; Kato, G. Tumor angiogenesis and novel antiangiogenic strategies. *Int. J. Cancer* **2010**, *126* (8), 1777–87.

(6) Pollard, J. W. Macrophages define the invasive microenvironment in breast cancer. *J. Leukoc. Biol.* **2008**, *84* (3), 623–30.

(7) Vona-Davis, L.; Rose, D. P. Angiogenesis, adipokines and breast cancer. *Cytokine Growth Factor Rev.* **2009**, *20* (3), 193–201.

(8) Chen, S. T.; Pan, T. L.; Juan, H. F.; Chen, T. Y.; Lin, Y. S.; Huang, C. M. Breast tumor microenvironment: proteomics highlights the treatments targeting secretome. *J. Proteome Res.* **2008**, *7* (4), 1379–87.

(9) Johann, D. J.; Rodriguez-Canales, J.; Mukherjee, S.; Prieto, D. A.; Hanson, J. C.; Emmert-Buck, M.; Blonder, J. Approaching solid tumor heterogeneity on a cellular basis by tissue proteomics using laser capture microdissection and biological mass spectrometry. *J. Proteome Res.* **2009**, *8* (5), 2310–8.

(10) Griffin, N. M.; Schnitzer, J. E. Chapter 8. Proteomic mapping of the vascular endothelium in vivo for vascular targeting. *Methods Enzymol.* **2008**, *445*, 177–208.

(11) Mustafa, D. A.; Burgers, P. C.; Dekker, L. J.; Charif, H.; Titulaer, M. K.; Smitt, P. A.; Luider, T. M.; Kros, J. M. Identification of glioma neovascularization-related proteins by using MALDI-FTMS and nano-LC fractionation to microdissected tumor vessels. *Mol. Cell. Proteomics* **2007**, *6* (7), 1147–57.

(12) Simonson, A. B.; Schnitzer, J. E. Vascular proteomic mapping in vivo. *J. Thromb. Haemost.* **2007**, *5* (Suppl 1), 183–7.

(13) Domazet, B.; Maclennan, G. T.; Lopez-Beltran, A.; Montironi, R.; Cheng, L. Laser capture microdissection in the genomic and proteomic era: targeting the genetic basis of cancer. *Int. J. Clin. Exp. Pathol.* **2008**, *1* (6), 475–88.

(14) Cha, S.; Imielinski, M. B.; Rejtar, T.; Richardson, E. A.; Thakur, D.; Sgroi, D. C.; Karger, B. L. In situ proteomic analysis of human breast cancer epithelial cells using laser capture microdissection: annotation by protein set enrichment analysis and gene ontology. *Mol. Cell. Proteomics* **2010**, *9* (11), 2529–44.

(15) Umar, A.; Kang, H.; Timmermans, A. M.; Look, M. P.; Meijer-van Gelder, M. E.; den Bakker, M. A.; Jaitly, N.; Martens, J. W.; Luider, T. M.; Foekens, J. A.; Pasa-Tolic, L. Identification of a putative protein profile associated with tamoxifen therapy resistance in breast cancer. *Mol. Cell. Proteomics* **2009**, *8* (6), 1278–94.

(16) Pen, A.; Moreno, M. J.; Martin, J.; Stanimirovic, D. B. Molecular markers of extracellular matrix remodeling in glioblastoma vessels: microarray study of laser-captured glioblastoma vessels. *Glia* **2007**, *55* (6), 559–72.

(17) Bhati, R.; Patterson, C.; Livasy, C. A.; Fan, C.; Ketelsen, D.; Hu, Z.; Reynolds, E.; Tanner, C.; Moore, D. T.; Gabrielli, F.; Perou, C. M.; Klauber-DeMore, N. Molecular characterization of human breast tumor vascular cells. *Am. J. Pathol.* **2008**, *172* (5), 1381–90.

(18) Murugesan, N.; Macdonald, J. A.; Lu, Q.; Wu, S. L.; Hancock, W. S.; Pachter, J. S. Analysis of mouse brain microvascular endothelium using laser capture microdissection coupled with proteomics. *Methods Mol. Biol.* **2011**, *686*, 297–311.

(19) Haqqani, A. S.; Nesic, M.; Preston, E.; Baumann, E.; Kelly, J.; Stanimirovic, D. Characterization of vascular protein expression patterns in cerebral ischemia/reperfusion using laser capture microdissection and ICAT-nanoLC-MS/MS. *Faseb J.* **2005**, *19* (13), 1809–21.

(20) Lu, Q.; Murugesan, N.; Macdonald, J. A.; Wu, S. L.; Pachter, J. S.; Hancock, W. S. Analysis of mouse brain microvascular endothelium using immuno-laser capture microdissection coupled to a hybrid linear ion trap with Fourier transform-mass spectrometry proteomics platform. *Electrophoresis* **2008**, *29* (12), 2689–95.

(21) Johann, D. J., Jr.; Wei, B. R.; Prieto, D. A.; Chan, K. C.; Ye, X.; Valera, V. A.; Simpson, R. M.; Rudnick, P. A.; Xiao, Z.; Issaq, H. J.; Linehan, W. M.; Stein, S. E.; Veenstra, T. D.; Blonder, J. Combined blood/tissue analysis for cancer biomarker discovery: application to renal cell carcinoma. *Anal. Chem.* **2010**, *82* (5), 1584–8.

(22) Unwin, R. D.; Craven, R. A.; Harnden, P.; Hanrahan, S.; Totty, N.; Knowles, M.; Eardley, I.; Selby, P. J.; Banks, R. E. Proteomic changes in renal cancer and co-ordinate demonstration of both the glycolytic and mitochondrial aspects of the Warburg effect. *Proteomics* **2003**, *3* (8), 1620–32.

(23) Palagi, P. M.; Walther, D.; Quadroni, M.; Catherinet, S.; Burgess, J.; Zimmermann-Ivol, C. G.; Sanchez, J. C.; Binz, P. A.; Hochstrasser, D. F.; Appel, R. D. MSight: an image analysis software for liquid chromatography-mass spectrometry. *Proteomics* **2005**, *5* (9), 2381–4.

(24) Hill, J. J.; Moreno, M. J.; Lam, J. C.; Haqqani, A. S.; Kelly, J. F. Identification of secreted proteins regulated by cAMP in glioblastoma cells using glycopeptide capture and label-free quantification. *Proteomics* **2009**, *9* (3), 535–49.

(25) Haqqani, A. S.; Kelly, J. F.; Stanimirovic, D. B. Quantitative protein profiling by mass spectrometry using label-free proteomics. *Methods Mol. Biol.* **2008**, *439*, 241–56.

(26) Miller, L. D.; Smeds, J.; George, J.; Vega, V. B.; Vergara, L.; Ploner, A.; Pawitan, Y.; Hall, P.; Klaar, S.; Liu, E. T.; Bergh, J. An expression signature for p53 status in human breast cancer predicts mutation status, transcriptional effects, and patient survival. *Proc. Natl. Acad. Sci. U.S.A.* **2005**, *102* (38), 13550–5.

(27) Chang, H. Y.; Nuyten, D. S.; Sneddon, J. B.; Hastie, T.; Tibshirani, R.; Sorlie, T.; Dai, H.; He, Y. D.; van't Veer, L. J.; Bartelink, H.; van de Rijn, M.; Brown, P. O.; van de Vijver, M. J. Robustness, scalability, and integration of a wound-response gene expression signature in predicting breast cancer survival. *Proc. Natl. Acad. Sci. U.S.A.* **2005**, *102* (10), 3738–43.

(28) Wang, Y.; Klijn, J. G.; Zhang, Y.; Sieuwerts, A. M.; Look, M. P.; Yang, F.; Talantov, D.; Timmermans, M.; Meijer-van Gelder, M. E.; Yu, J.; Jatkoe, T.; Berns, E. M.; Atkins, D.; Foekens, J. A. Gene-expression profiles to predict distant metastasis of lymph-node-negative primary breast cancer. *Lancet* **2005**, *365* (9460), 671–9.

(29) Cui, Q.; Ma, Y.; Jaramillo, M.; Bari, H.; Awan, A.; Yang, S.; Zhang, S.; Liu, L.; Lu, M.; O'Connor-McCourt, M.; Purisima, E. O.; Wang, E. A map of human cancer signaling. *Mol. Syst. Biol.* **2007**, *3*, 152.

(30) Li, J.; Lenferink, A. E.; Deng, Y.; Collins, C.; Cui, Q.; Purisima, E. O.; O'Connor-McCourt, M. D.; Wang, E. Identification of high-quality cancer prognostic markers and metastasis network modules. *Nat. Commun.* **2010**, *1*, 34.

(31) Holthofer, H.; Virtanen, I.; Kariniemi, A. L.; Hormia, M.; Linder, E.; Miettinen, A. Ulex europaeus I lectin as a marker for vascular endothelium in human tissues. *Lab. Invest.* **1982**, *47* (1), 60–6.

(32) Hormia, M.; Lehto, V. P.; Virtanen, I. Identification of UEA I-binding surface glycoproteins of cultured human endothelial cells. *Cell Biol. Int. Rep.* **1983**, *7* (6), 467–75.

(33) Blonder, J.; Conrads, T. P.; Yu, L. R.; Terunuma, A.; Janini, G. M.; Issaq, H. J.; Vogel, J. C.; Veenstra, T. D. A detergent- and cyanogen bromide-free method for integral membrane proteomics: application to Halobacterium purple membranes and the human epidermal membrane proteome. *Proteomics* **2004**, *4* (1), 31–45.

(34) Blonder, J.; Chan, K. C.; Issaq, H. J.; Veenstra, T. D. Identification of membrane proteins from mammalian cell/tissue using methanol-facilitated solubilization and tryptic digestion coupled with 2D-LC-MS/MS. *Nat. Protoc.* **2006**, *1* (6), 2784–90.

(35) Johnson, M.; Sharma, M.; Henderson, B. R. IQGAP1 regulation and roles in cancer. *Cell Signal.* **2009**, *21* (10), 1471–8.

(36) Yonenaga, Y.; Mori, A.; Onodera, H.; Yasuda, S.; Oe, H.; Fujimoto, A.; Tachibana, T.; Imamura, M. Absence of smooth muscle actin-positive pericyte coverage of tumor vessels correlates with hematogenous metastasis and prognosis of colorectal cancer patients. *Oncology* **2005**, *69* (2), 159–66.

(37) Shao, R.; Bao, S.; Bai, X.; Blanchette, C.; Anderson, R. M.; Dang, T.; Gishizky, M. L.; Marks, J. R.; Wang, X. F. Acquired expression of periostin by human breast cancers promotes tumor angiogenesis through up-regulation of vascular endothelial growth factor receptor 2 expression. *Mol. Cell. Biol.* **2004**, *24* (9), 3992–4003.

(38) Orend, G.; Chiquet-Ehrismann, R. Tenascin-C induced signaling in cancer. *Cancer Lett* **2006**, *244* (2), 143–63.

(39) Ricciardelli, C.; Sakko, A. J.; Ween, M. P.; Russell, D. L.; Horsfall, D. J. The biological role and regulation of versican levels in cancer. *Cancer Metastasis Rev.* **2009**, *28* (1−2), 233–45.

(40) Lin, C. S.; Park, T.; Chen, Z. P.; Leavitt, J. Human plastin genes. Comparative gene structure, chromosome location, and differential expression in normal and neoplastic cells. *J. Biol. Chem.* **1993**, *268* (4), 2781–92.

(41) Zheng, P. P.; Severijnen, L. A.; van der Weiden, M.; Willemsen, R.; Kros, J. M. A crucial role of caldesmon in vascular development in vivo. *Cardiovasc. Res.* **2009**, *81* (2), 362–9.

(42) Tang, J.; Hu, G.; Hanai, J.; Yadlapalli, G.; Lin, Y.; Zhang, B.; Galloway, J.; Bahary, N.; Sinha, S.; Thisse, B.; Thisse, C.; Jin, J. P.; Zon, L. I.; Sukhatme, V. P. A critical role for calponin 2 in vascular development. *J. Biol. Chem.* **2006**, *281* (10), 6664–72.

(43) Baluk, P.; Morikawa, S.; Haskell, A.; Mancuso, M.; McDonald, D. M. Abnormalities of basement membrane on blood vessels and endothelial sprouts in tumors. *Am. J. Pathol.* **2003**, *163* (5), 1801–15.

(44) Reinboth, B.; Thomas, J.; Hanssen, E.; Gibson, M. A. Beta ig-h3 interacts directly with biglycan and decorin, promotes collagen VI aggregation, and participates in ternary complexing with these macromolecules. *J. Biol. Chem.* **2006**, *281* (12), 7816–24.

(45) Sauk, J. J.; Nikitakis, N.; Siavash, H. Hsp47 a novel collagen binding serpin chaperone, autoantigen and therapeutic target. *Front. Biosci.* **2005**, *10*, 107–18.

(46) Kazerounian, S.; Yee, K. O.; Lawler, J. Thrombospondins in cancer. *Cell. Mol. Life Sci.* **2008**, *65* (5), 700–12.

(47) Chen, C. D.; Wang, C. S.; Huang, Y. H.; Chien, K. Y.; Liang, Y.; Chen, W. J.; Lin, K. H. Overexpression of CLIC1 in human gastric carcinoma and its clinicopathological significance. *Proteomics* **2007**, *7* (1), 155–67.

(48) Petrova, D. T.; Asif, A. R.; Armstrong, V. W.; Dimova, I.; Toshev, S.; Yaramov, N.; Oellerich, M.; Toncheva, D. Expression of chloride intracellular channel protein 1 (CLIC1) and tumor protein D52 (TPD52) as potential biomarkers for colorectal cancer. *Clin. Biochem.* **2008**, *41* (14−15), 1224–36.

(49) Chang, Y. H.; Wu, C. C.; Chang, K. P.; Yu, J. S.; Chang, Y. C.; Liao, P. C. Cell secretome analysis using hollow fiber culture system leads to the discovery of CLIC1 protein as a novel plasma marker for nasopharyngeal carcinoma. *J. Proteome Res.* **2009**, *8* (12), 5465–74.

(50) Wang, J. W.; Peng, S. Y.; Li, J. T.; Wang, Y.; Zhang, Z. P.; Cheng, Y.; Cheng, D. Q.; Weng, W. H.; Wu, X. S.; Fei, X. Z.; Quan, Z. W.; Li, J. Y.; Li, S. G.; Liu, Y. B. Identification of metastasis-associated proteins involved in gallbladder carcinoma metastasis by proteomic analysis and functional exploration of chloride intracellular channel 1. *Cancer Lett.* **2009**, *281* (1), 71–81.

(51) Ulmasov, B.; Bruno, J.; Gordon, N.; Hartnett, M. E.; Edwards, J. C. Chloride intracellular channel protein-4 functions in angiogenesis by supporting acidification of vacuoles along the intracellular tubulogenic pathway. *Am. J. Pathol.* **2009**, *174* (3), 1084–96.

(52) Tung, J. J.; Kitajewski, J. Chloride intracellular channel 1 functions in endothelial cell growth and migration. *J. Angiogenes Res.* **2010**, *2*, 23.

(53) Insall, R. H.; Machesky, L. M. Actin dynamics at the leading edge: from simple machinery to complex networks. *Dev. Cell* **2009**, *17* (3), 310–22.

(54) Olson, M. F.; Sahai, E. The actin cytoskeleton in cancer cell motility. *Clin. Exp. Metastasis* **2009**, *26* (4), 273–87.

(55) Yamaoka-Tojo, M.; Ushio-Fukai, M.; Hilenski, L.; Dikalov, S. I.; Chen, Y. E.; Tojo, T.; Fukai, T.; Fujimoto, M.; Patrushev, N. A.; Wang, N.; Kontos, C. D.; Bloom, G. S.; Alexander, R. W. IQGAP1, a novel vascular endothelial growth factor receptor binding protein, is involved in reactive oxygen species--dependent endothelial migration and proliferation. *Circ. Res.* **2004**, *95* (3), 276–83.

(56) Gonzalez, A. M.; Otey, C.; Edlund, M.; Jones, J. C. Interactions of a hemidesmosome component and actinin family members. *J. Cell Sci.* **2001**, *114* (Pt 23), 4197–206.

(57) Janke, J.; Schluter, K.; Jandrig, B.; Theile, M.; Kolble, K.; Arnold, W.; Grinstein, E.; Schwartz, A.; Estevez-Schwarz, L.; Schlag, P. M.; Jockusch, B. M.; Scherneck, S. Suppression of tumorigenicity in breast cancer cells by the microfilament protein profilin 1. *J. Exp. Med.* **2000**, *191* (10), 1675–86.

(58) Zou, L.; Jaramillo, M.; Whaley, D.; Wells, A.; Panchapakesa, V.; Das, T.; Roy, P. Profilin-1 is a negative regulator of mammary carcinoma aggressiveness. *Br. J. Cancer* **2007**, *97* (10), 1361–71.

(59) Wu, K. C.; Jin, J. P. Calponin in non-muscle cells. *Cell Biochem. Biophys.* **2008**, *52* (3), 139–48.

(60) Xu, S. G.; Yan, P. J.; Shao, Z. M. Differential proteomic analysis of a highly metastatic variant of human breast cancer cells using two-dimensional differential gel electrophoresis. *J. Cancer Res. Clin. Oncol.* **2010**, *136* (10), 1545–56.

(61) Saeed, A. I.; Sharov, V.; White, J.; Li, J.; Liang, W.; Bhagabati, N.; Braisted, J.; Klapa, M.; Currier, T.; Thiagarajan, M.; Sturn, A.; Snuffin, M.; Rezantsev, A.; Popov, D.; Ryltsov, A.; Kostukovich, E.; Borisovsky, I.; Liu, Z.; Vinsavich, A.; Trush, V.; Quackenbush, J. TM4: a free, open-source system for microarray data management and analysis. *Biotechniques* **2003**, *34* (2), 374–8.